# Nanoscale

Accepted Manuscript


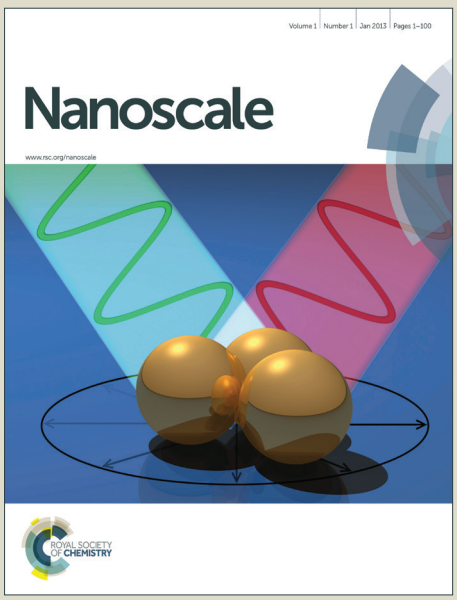





ROYAL SOCIETY OF CHEMISTRY

www.rsc.org/nanoscale

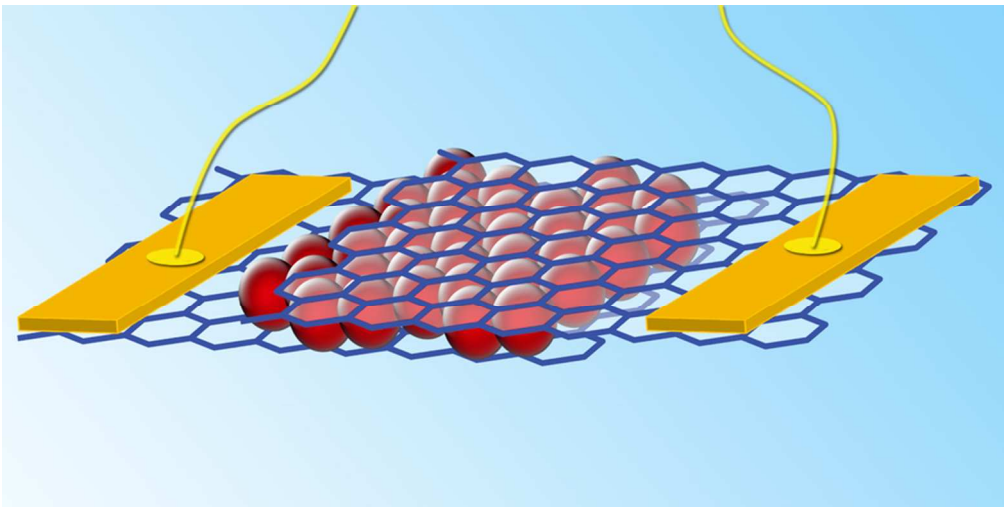

The fabrication and characterization of a vertical heterostructure composed of van der Waals and nanoparticle monolayers, the graphene/CdSe nanoparticle monolayer/graphene sandwich, is presented.
40x20mm (600 x 600 DPI)

The fabrication and characterization of a vertical heterostructure composed of van der Waals and nanoparticle monolayers, the graphene/CdSe nanoparticle monolayer/graphene sandwich, is presented.

Nanoscale

RSCPublishing

COMMUNICATION

# Electronic Transport in Nanoparticle Monolayers Sandwiched Between Graphene Electrodes

Cite this: DOI: 10.1039/x0xx00000x

Chenguang Lu,*[a] Datong Zhang,[b] Arend van der Zande,[c] Philip Kim,[d] and Irving P. Herman*[b]

Received 00th January 2012,
Accepted 00th January 2012

DOI: 10.1039/x0xx00000x

www.rsc.org/nanoscale

**Graphene/CdSe nanoparticle monolayer/graphene sandwich structures were fabricated to explore the interactions between these layered materials. Electrical transport across these heterostructures suggests that transport is limited by tunneling through the nanoparticle (NP) ligands but not the NP core itself. Photoconductivity suggests ligands may affect the exciton separation efficiency.**

Two-dimensional (2D) materials, such as graphene, boron nitride, $MoS_2$, etc. have attracted much attention due to their unique properties. Stacking these van der Waals (vdW) monolayers (MLs) vertically into so-called vdW materials or heterostructures[1] can produce materials with new properties and functionalities due to the interactions between the vdW MLs. Field effect tunneling transistors,[2] barristors[3] and prototypical solar cell devices[2] have been demonstrated by using this design concept. However, the building blocks used in such structures are limited to the few types of vdW MLs, and these have band structures that are difficult to modify for engineering purposes. The current vertical stacking technique also limits the thickness of each layer and the possibilities for scaled-up production of these types of devices. It would be desirable to devise a class of building blocks with tunable properties and scalable stacking control to enrich the properties of assembled materials and broaden potential applications of this design concept.

Nanoparticles (NPs) with size-dependent properties have been investigated for more than 20 years.[4-6] The ability to produce monolayer, ordered films of monodisperse NPs[7,8] opens the possibility of incorporating NP MLs with tunable properties into vdW materials. One could adjust the size, shape, composition, and ligands of the NPs to obtain NP MLs with versatile properties. Here, we demonstrate the fabrication of vdW ML/NP ML/vdW ML "sandwiches", with self-assembled CdSe NP monolayers between graphene MLs, and investigate the transport properties of these vertical heterostructures. Given the flexibility in choosing NPs, these sandwich heterostructures constitute a new category of 2D material with various properties that can be engineered. Previous work on interfacing NPs and vdW MLs has included that with individual NPs and drop-cast, disordered NP films on the vdW MLs.[9,10]

CdSe nanoparticles with 3.5 nm diameter cores were synthesized with a well-established method.[11] These as-made NPs were highly monodisperse, <5% dispersion, as confirmed by transmission electron microscopy (TEM) and ultraviolet-visible (UV-Vis) absorption methods, and were used without further size selection. The NP ligands were oleates, after ligand exchange using oleic acid, as demonstrated in Ref. 12 (see the Supplementary Information).

The heterostructures were fabricated as depicted in Fig. 1a. Monolayers of graphene were placed on top of Si wafers with 300 nm of thermally-grown oxide by the "scratching" method, and electrodes were attached to them (see the Supplementary Information). The 3.5 nm diameter CdSe NPs (capped with oleates) were dispersed in a hexane:decane (9:1) mixture solvent and 100 μL of this solution was drop-cast on top of a dimethyl sulfoxide (DMSO) subphase, with ~10 $cm^2$ area.[13,14] The hexane:decane solvent and the more-dense DMSO are immiscible. The upper hexane:decane phase was allowed to evaporate and NPs formed a film that floated on top of the DMSO phase. The concentration of drop-cast NPs was adjusted to obtain an NP monolayer. The NP MLs extended laterally up to several mm and were free of vacancies as was confirmed locally (~10 μm) by TEM (see Supplementary Information Fig. S2). The wafer with graphene was used to scoop up the NP layer on top of the DMSO, so the NP ML covered the entire graphene piece, and then the residual DMSO was allowed to evaporate in a glove box.[14] A second graphene ML was then mechanically transferred on top of the NP ML, to complete the graphene/CdSe NP ML/graphene vertical heterostructure sandwich, and then metal electrodes were attached to this upper graphene piece. Details of the techniques for scratching and transferring graphene are in the Supplementary Information, along with the use of e-beam lithography to define metal electrodes after the transfer of each graphene ML. (Two electrodes were attached to each graphene layer; one on each was used to measure transport across the sandwich and both were used to probe transport across each graphene ML, as in some back gate dependence measurements.)

Fig. 1c shows an optical image of one set of devices. The top graphene layer sometimes rolled up after transfer in several of the samples (not shown) (see the Supplementary information). We believe this is due to the poor adhesion between graphene and the organic ligands that coat the NPs. (Better surface chemistry control could address this issue and is under investigation.)

The *I-V* characteristics of all of the structurally sound devices were measured at room temperature, first with no back gate voltage.

A typical current-voltage (*I-V*) curve of one of the seven working devices is shown in Fig. 2a. All *I-V* profiles had approximately the same shape. (Shorting in the other structures (see the Supplementary Information about device yield) is perhaps due to graphene-graphene shorting across an NP ML vacancy that developed during transfer. Working devices continued to work in vacuum, but shorted when cooled to 250 K, presumably due to fracture of the NP film and resulting contact of the two graphene layers, and remained shorted when warmed to room temperature.)

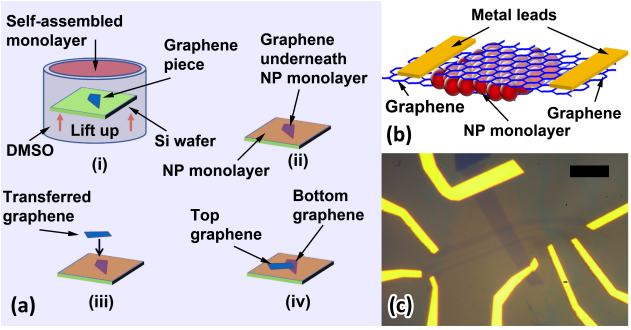


**Fig. 1** (a) Schematic depicting the fabrication the graphene/NP ML/graphene sandwich structure, with the exfoliation of the bottom graphene layer on the substrate occurring before step (i). (b) Schematic illustration of the structure of the device. (c) An optical image of one set of three such devices, with the three thin graphene pieces of the bottom graphene later made by oxygen plasma etching. The scale bar in (c) is 10 μm wide.

Gate voltage, $V_g$, was applied through the back Si gate for this device (Fig. 2b) and several other working devices; no strong dependence on the gate voltage was seen. This suggests that the graphene layer may be in the heavy doping regime. This was confirmed by measuring the current across both the top and the bottom graphene layer while sweeping $V_g$ (see Supplementary Information Fig. S4b, and Raman measurements in Fig. S5);[15] no evidence for a Dirac point for either graphene ML was observed. Air exposure could cause such p-doping because of $O_2$ adsorption. However, the level of doping is much higher in our devices than in Refs. 15 and 16, which cannot be explained by $O_2$ adsorption alone. We attribute this heavy doping to the adsorption of the carboxylic group of the ligand, which is highly polar and could withdraw electrons from the graphene layers. We believe that when the NP ML forms after hexane:decane evaporation, some unbound ligands (in solution, which are in equilibrium with the ligands on the NP cores[12]) deposit on top of the NP ML and may dope the graphene layers, with their polar groups when they were brought into contact.

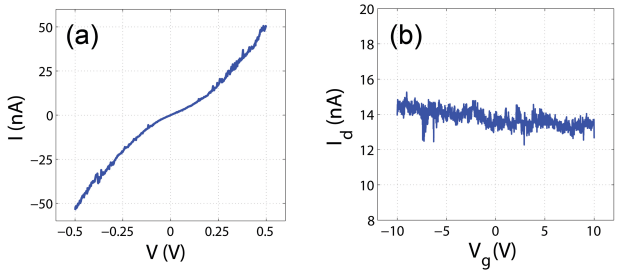


**Fig. 2** (a) *I-V* curve of one graphene/CdSe NP ML/graphene device. (b) $I_{ds}$-$V_g$ curve of this device ($V_{ds}$ = 0.2 V), showing a weak gate dependence, which suggests heavy doping of the graphene layers.

*I-V* sweeps of our devices show a tunneling type of conduction similar to that observed previously in tunneling from a graphene electrode, through a vdW barrier, and to a second graphene electrode.[2,17,18] The tunneling current can be modeled by using the Bardeen transfer Hamiltonian approach,[2,17,18] with

$$I \propto \int dE\, DoS_B(E) DoS_T(E + eV_i) \cdot [f(E) - f(E + eV_i)] \cdot T(E, V_i), \quad (1)$$

where $E$ is the energy of electrons with respect to the Dirac point of the bottom graphene; $V_i$ is the voltage drop across the tunneling barrier, which is equal to the potential difference between the Dirac points of the graphene layers (and which depends on the applied drain-source voltage, $V_{ds}$); $DoS_{B,T}$ are the densities of states of the bottom and top graphene layers (which we use in approximate form, $2|E|/(\pi(\hbar v_F)^2)$, near the Dirac point), respectively; $f(E)$ is the Fermi-Dirac function; and $T(E, V_i)$ is the tunneling probability.

The capacitance of the graphene layers affects how $\boldsymbol{V_{ds}}$ is distributed across the stacked layers. We expect that $\boldsymbol{V_i}$ is smaller than $\boldsymbol{V_{ds}}$, and an appreciable amount of the voltage drop is within the graphene layers, considering the quantum capacitance of graphene electrodes. Since graphene has a small density of states near the Dirac point, accumulated charges on the graphene electrodes due to the capacitive charging between the electrode can shift the quasi Fermi level considerably. The charge induced by $\boldsymbol{V_i}$, especially at high bias, changes the Fermi level of graphene and consequently redistributes the voltage drop throughout the system.[19]

The $V_i$ across the graphene layers and the Fermi level shifts of each graphene ML, $\Delta E_B$ and $\Delta E_T$ for the bottom and top graphene, are determined self-consistently for any given $V_{ds}$ by using:

$$eV_{ds} = eV_i + \Delta E_B - \Delta E_T \quad (2)$$

$$CV_i = \int_{-\infty}^{+\infty} DoS(E)(f(E - \mu_B - \Delta E_B) - f(E - \mu_B))\, dE \quad (3)$$

$$-CV_i = \int_{-\infty}^{+\infty} DoS(E)\big(f(E - \mu_T - \Delta E_T) - f(E - \mu_T)\big)\, dE, \quad (4)$$

where $\mu_B$ and $\mu_T$ are the chemical potentials of the bottom and top graphene pieces with no voltage applied, and the effective capacitance of the CdSe cores and ligands is modeled (in a simplified, approximate manner) as

$$C = \left(\frac{t_{core}}{\varepsilon_0 \varepsilon_{CdSe}} + \frac{t_{shell}}{\varepsilon_0 \varepsilon_{decane}}\right)^{-1}, \quad (5)$$

where $\varepsilon_0$ is the permittivity of free space, and the dielectric constants of bulk CdSe, $\varepsilon_{CdSe}$, (for the CdSe core) and typical alkane chains, $\varepsilon_{decane}$, (for the ligands)[20] are used along with the diameter of the NP core, $t_{core}$, and the effective total thickness of the ligands (on opposing sides of the core), $t_{shell}$.

The tunneling probability $T(E, V_i)$ is determined using an expression similar to the WKB approximation by Britnell et al.,[1] with

$$T(E, V_i) = \exp\left[-\frac{2\sqrt{2m^*}}{\hbar}\int_0^d dx \sqrt{(\Delta - E) - \frac{eV_i x}{d}}\right], \quad (6)$$

where $m^*$ is the electron effective mass inside the barrier, Δ is the effective barrier height at flat band with respect to the Dirac point of the bottom graphene, and $d$ is the effective barrier thickness.

The *I-V* curves of all devices can be fit using this model only for barrier thicknesses thinner than 2.5 nm (when using the reasonable assumption that the electron effective mass > 0.1 $m_e$), which is significantly smaller than the 3.5 nm CdSe NP core diameter. This is illustrated in Fig. 3a in which the barrier thickness is set to 4.5 nm



 

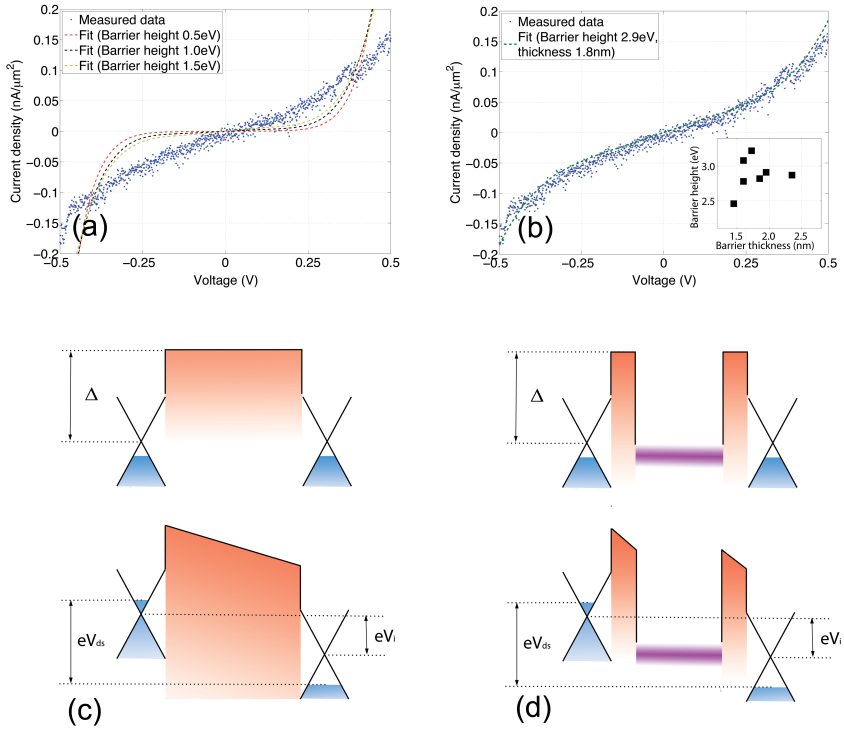


**Fig. 3** (a) Fit of one measured *I-V* curve (for the device also depicted in Fig. S4) with barrier thickness 4.5 nm and various barrier heights, suggesting that no good fit can be achieved with a reasonable barrier height for larger barrier widths and that the CdSe NP core is not the major barrier. (b) Fit *I-V* curve for this device, with the inset showing the fit barrier heights and thicknesses of all seven devices, using least squares analysis. (The current densities are plotted in (a) and (b).) Schematic of the tunneling barriers between the graphene layers for an effective barrier in (c) and the ligand barriers on either side of the NP core in (d). Δ is the barrier height.

(NP core diameter 3.5 nm plus the ligand thickness ~1.0 nm); the *I-V* curves (for the device depicted in Fig. S4 in the Supplementary Information), cannot be fit with this model for any barrier height. This suggests that the CdSe NP cores are not the major tunneling barrier between the two graphene layers, which is consistent with expectations from band alignment. The conduction band of CdSe NPs with a similar size cores nearly lines up with the graphene Dirac point, i.e. about 4.5 V below the vacuum level,[21,22] so the graphene out-of-plane wave function is not expected to decay significantly within the cores of CdSe NPs. There were no resonance features attributable to states of the CdSe NP cores, likely due to the "high" measurement temperature (room temperature) and the (small, but finite) inhomogeneity in the sizes of the CdSe cores.

Consequently, we believe the ligands on the CdSe NP cores are the major tunneling barriers in this case. Studies of self-assembled alkane chains have shown a tunneling behavior[23,24] similar to that seen in our devices. In the standard regime of electron tunneling through a self-assembled alkane monolayer, the tunneling probability can be expressed in a WKB form, with an electron effective mass of 0.42 $m_e$.[23,24]

The *I-V* curve of each device was fit using an effective barrier height Δ and thickness *d* as fitting parameters. The data and the fit for the device studied in Fig. S4 in the Supplementary Information are shown in Fig. 3b. The fit for each device is plotted in the inset; the averages of these fits gives $\Delta = 2.88 \pm 0.24$ eV and $d = 1.89 \pm 0.30$ nm. (More details on the fitting procedure are provided in the Supplementary Information.)

We also measured the photoconductivity of our device under illumination by a cw 532 nm laser (9 μW, ~1 μm spot size), for $V_{ds}$ = 0.25 V and no back gate voltage. Fig. 4b shows the 2D map of the photoconductivity response of the device shown in Fig. 4a, along with the borders of the graphene electrodes that are also seen in Fig. 4a. This response is plotted in Fig. 4c for the region spanned by the chosen lower electrode (averaged in the normal direction within this region outlined in Fig. 4a). This device exhibits an appreciable response from only the right half of the overlap region. Electronic transport through the device may be the largest there and the organic ligand barrier may be thicker in the other half, which also suggests the needs for better control of the NP surface chemistry. Photoconductivity increases the measured current by ~0.8 nA in regions where the NP and two graphene MLs overlap. We estimate the upper limit of the exciton-induced current increase to be ~7.0 nA, as described in the Supplementary Information. The conversion of absorbed photons to charges suggests that most excitons are not extracted by the bias voltage and recombine inside the NPs, likely due to the long tunneling lifetime associated with the NP ligands.

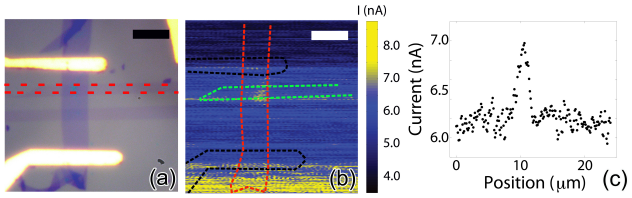


**Fig. 4** (a) Optical image of a sandwich device. The bright yellow leads are the gold electrodes connected to the top graphene layer, which is the vertical blue stripe. The two horizontal light blue stripes are the bottom graphene pieces; the upper one is used in this measurement. (b) The 2D photocurrent mapping signals under 0.25 V bias for a scanning 532 nm laser with spot size ~1 μm and power 9 μW. (c) The photocurrent in (b) is averaged vertically within the red dashed line box in (a) and plotted along the horizontal

dimension of this box. The maximum photon-induced current is ~0.8 nA. The scale bars are 5 μm wide in (a) and (b).

## Conclusions

In summary, we have assembled a novel vertical heterostructure, a graphene ML/CdSe nanoparticle ML/graphene ML sandwich, which is prototypical of a new family of 2D van der Waals materials with tunable properties. The readily scalable production of NP monolayers, together with mass production of 2D materials,[25,26] can enable scaling-up the fabrication of these structures when necessary. Measurements show that transport across these particular sandwich devices is limited by tunneling through the nanoparticle ligands rather than its core, with an effective barrier height of 2.88 ± 0.24 eV and barrier thickness of 1.89 ± 0.30 nm.

Surface chemistry control of the nanoparticles, to shorter ligands or decomposable ligands, is expected to bring the cores closer and may enable properties that are dependent on strong inter-core interactions, and with limited exciton recombination in photon-excited sandwiches. Photoconductivity measurements show that exciton extraction may also be limited by the NP ligands, which is another motivation for removing or shortening these ligands. Studies of NP ligand exchange are underway in order to bring the NP cores closer to the top and bottom graphene layers. Sandwich devices fabricated using other vdW MLs, such as $MoS_2$, are also under investigation.

## Acknowledgements

Author 1 and Author 2 contributed equally to this work. We thank Jonathan Liu, Fereshte Ghahari, and Michael Landry for assistance with sample preparation. Support was provided by the MIRT program of the National Science Foundation (DMR-1122594) and the EFRC program of DoE (DE-SC0001085), by the New York State Office of Science, Technology, and Academic Research, and a gift by the Honda Research Institute. Use of the National Synchrotron Light Source (NSLS), Brookhaven National Laboratory, was supported by the U.S. Department of Energy, Office of Science, Office of Basic Energy Sciences, under contract no. DE-AC02-98CH10886. We thank Drs. Lin Yang and Masafumi Fukuto for their assistance at the NSLS X9A beamline.

## Notes and references

[a] Department of Applied Physics and Applied Mathematics, Columbia University, New York, NY 10027, USA; National Center for Nanoscience and Technology, Beijing 100190, China. E-mail: lucg@nanoctr.cn
[b] Department of Applied Physics and Applied Mathematics, Columbia University, New York, NY 10027, USA. E-mail: iph1@columbia.edu
[c] Energy Frontier Research Center, Department of Mechanical Engineering, Columbia University, New York, NY 10027, USA.
[d] Department of Physics, Columbia University, New York, NY 10027, USA.; current address: Department of Physics, Harvard University, Cambridge, MA 02138, USA.

† Electronic Supplementary Information (ESI) available. See DOI: 10.1039/c000000x/

1 A. K. Geim and I. V. Grigorieva, *Nature,* 2013, **499**, 419.
2 L. Britnell, R. V. Gorbachev, R. Jalil, B.D. Belle, F. Schedin, A. Mishchenko, T. Georgiou, M. I. Katsnelson, L. Eaves, S. V. Morozov, N. M. R. Peres, J. Leist, A. K. Geim, K. S. Novoselov and L. A. Ponomarenko, *Science,* 2012, **335**, 947.
3 H. Yang, J. Heo, S. Park, H. J. Song, D. H. Seo, K. E. Byun, P. Kim, I. Yoo, H. J. Chung and K. Kim, *Science*, 2012, **336**, 1140.
4 D. V. Talapin, J. S. Lee, M. V. Kovalenko and E. V. Shevchenko, *Chem. Rev.*, 2010, **110**, 389.
5 J. Park, J. Joo, S. G. Kwon, Y. Jang and T. Hyeon, *Angew. Chem. Int. Ed.*, 2007, **46**, 4630.
6 P. D. Cozzoli, T. Pellegrino and L. Manna, *Chem. Soc. Rev.*, 2006, **35**, 1195
7 V. Aleksandrovic, D. Greshnykh, I. Randjelovic, A. Froemsdorf, A. Kornowski, S. V. Roth, C. Klinke and H. Weller, *ACS Nano*, 2008, **2**, 1123.
8 Q. Guo, X. Teng, S. Rahman and H. Yang, *J. Am. Chem. Soc.*, 2002, **125**, 630.
9 Z. Chen, S. Berciaud, C. Nuckolls, T. F. Heinz and L. E. Brus, *ACS Nano*, 2010, **4**, 2964.
10 G. Konstantatos, M. Badioli, L. Gaudreau, J. Osmond, M. Bernechea, F. P. G. de Arquer, F. Gatti and F. H. L. Koppens, *Nature Nanotech.*, 2012, **7**, 363.
11 Z. A. Peng and X. Peng, *J. Am. Chem. Soc.*, 2000, **123**, 183.
12 X. Ji, D. Copenhaver, C. Sichmeller and X. Peng, *J. Am. Chem. Soc.*, 2008, **130**, 5726.
13 V. Aleksandrovic, D. Greshnykh, I. Randjelovic, A. Fromsdorf, A. Kornowski, S. V. Roth, C. Klinke and H. Weller, *ACS Nano*, 2008, **2**, 1123.
14 A. Dong, J. Chen, P. M. Vora, J. M. Kikkawa and C. B. Murray, *Nature*, 2010, **466**, 474.
15 B. Guo, Q. Liu, E. Chen, H. Zhu, L. Fang and J. R. Gong, *Nano Lett.*, 2010, **10**, 4975.
16 Y. W. Tan, Y. Zhang, K. Bolotin, Y. Zhao, S. Adam, E. H. Hwang, S. Das Sarma, H. L. Stormer and P. Kim, *Phys. Rev. Lett.*, 2007, **99**, 246803.
17 T. Georgiou, R. Jalil, B. D. Belle, L. Britnell, R. V. Gorbachev, S. V. Morozov, Y. J. Kim, A. Gholinia, S. J. Haigh, O. Makarovsky, L. Eaves, L. Ponomarenko, A. K. Geim, K. Novoselov and A. Mishchenko, *Nature Nanotech.*, 2012, **8**, 100.
18 L. Britnell, R. V. Gorbachev, R. Jalil, B. D. Belle, F. Schedin, M. I. Katsnelson, L. Eaves, S. V. Morozov, A. S. Mayorov, N. M. Peres, A. Castro Neto, J. Leist, A. K. Geim, L. Ponomarenko and K. Novoselov, *Nano Lett.*, 2012, **12**, 1707.
19 R. M. Feenstra, D. Jena and G. Gu, *J. Appl. Phys.*, 2012, **111**, 043711.
20 *CRC Handbook of Chemistry and Physics*; 94 ed.; Chemical Rubber Company, 2013.
21 M. Schlamp, X. Peng and A. Alivisatos, *J. Appl. Phys.*, 1997, **82**, 5837.
22 H. Mattoussi, L. H. Radzilowski, B. O. Dabbousi, E. L. Thomas, M. G. Bawendi and M. F. Rubner, *J. Appl. Phys.*, 1998, **83**, 7965.
23 W. Wang, T. Lee and M. A. Reed, *J. Phys. Chem. B*, 2004, **108**, 18398.
24 W. Wang, T. Lee and M. A. Reed, *Phys. Rev. B*, 2003, **68**, 035416.
25 Y. Hao, M. S. Bharathi, L. Wang, Y. Liu, H. Chen, S. Nie, X. Wang, H. Chou, C. Tan, B. Fallahazad, H. Ramanarayan, C. W. Magnuson, E. Tutuc, B. I. Yakobson, K. F. McCarty, Y. W. Zhang, P. Kim, J. Hone, L. Colombo and R. S. Ruoff, *Science*, 2013, **342**, 720.
26 X. Li, W. Cai, J. An, S. Kim, J. Nah, D. Yang, R. Piner, A. Velamakanni, I. Jung, E. Tutuc, S. K. Banerjee, L. Colombo and R. S. Ruoff, *Science*, 2009, **324**, 1312.



 